

Rapid Communication

2,2,6,6-Tetramethylpiperidine-1-oxyl acts as a volatile inhibitor of ferroptosis and neurological injury

Received 23 January 2022; accepted 27 April 2022; published online 3 May 2022

Hiroyuki Mizuno^{1,2}, Chisato Kubota^{1,*},
Yuta Takigawa³, Ryosuke Shintoku^{1,2},
Naokatsu Kannari⁴, Takako Muraoka⁵,
Hideru Obinata⁶, Yuhei Yoshimoto²,
Masato Kanazawa⁷, Ichiro Koshiishi^{3,8} and
Seiji Torii^{1,8,†}

¹Institute for Molecular and Cellular Regulation, Gunma University, Maebashi, Gunma 371-8512, Japan; ²Department of Neurosurgery, Gunma University Graduate School of Medicine, Maebashi, Gunma 371-8511, Japan; ³Department of Laboratory Sciences, Graduate School of Health Sciences, Gunma University, Maebashi, Gunma 371-8511, Japan; ⁴Department of Environmental Engineering Science, Graduate School of Science and Technology, Gunma University, Kiryu, Gunma 376-8515, Japan; ⁵Division of Molecular Science, Graduate School of Science and Technology, Gunma University, Kiryu, Gunma 376-8515, Japan; ⁶Education and Research Support Center, Gunma University Graduate School of Medicine, Maebashi, Gunma 371-8511, Japan; ⁷Department of Neurology, Brain Research Institute, Niigata University, Niigata 951-8585, Japan; and ⁸Center for Food Science and Wellness, Gunma University, Maebashi, Gunma 371-8511, Japan

*Present address: Takasaki University of Health and Welfare, Takasaki, Gunma, Japan

†Seiji Torii, Center for Food Science and Wellness, Gunma University, 3-39-22 Showa-machi, Maebashi 371-8511, Japan.
Tel./Fax: +81-27-220-8946, email: storii@gunma-u.ac.jp

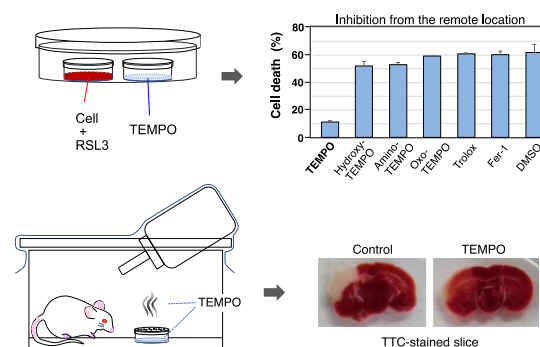
Ferroptosis, a type of oxidative stress cell death, has been implicated in cell injury in several diseases, and treatments with specific inhibitors have been shown to protect cells and tissues. Here we demonstrated that a treatment with the nitroxide radical, 2,2,6,6-tetramethylpiperidine-*N*-oxyl (TEMPO), prevented the ferroptotic cell death in an airborne manner. Other TEMPO derivatives and lipophilic antioxidants, such as Trolox and ferrostatin-1, also prevented cell death induced by erastin and RSL3; however, only TEMPO exhibited inhibitory activity from a physically distant location. TEMPO vaporized without decomposing and then dissolved again into a nearby water solution. Volatilized TEMPO inhibited glutamate-induced cell death in mouse hippocampal cell lines and also reduced neuronal cell death in a mouse ischemia model. These results suggest that TEMPO is a unique cell protective agent that acts in a volatility-mediated manner.

Keywords: gas; ischemia; lipid peroxidation; oxytosis; radical scavenger.

Introduction

Ferroptosis is regulated cell death induced by a number of stimuli, such as inhibition of glutathione biosynthesis or disruption of membrane peroxide-reducing systems (1, 2).

Graphical Abstract



This cellular event may be characterized at the molecular level by the accumulation of lethal lipid reactive oxygen species (ROS) in cell membranes, and at the morphological level by the appearance of shrunken mitochondria (3). The role of ferroptosis in cancer prevention and pathological cell death in ischemia and degenerative diseases has been extensively studied.

Glutathione peroxidase 4 (GPX4) is the primary suppressor of ferroptosis that can reduce lipid hydroperoxides even within membranes. The inactivation of GPX4 by the direct inhibition or depletion of glutathione has been shown to induce ferroptosis in several fibroblasts and cancer cells, and the inducible *Gpx4* deletion in mice led to cell death in the kidneys, brain, retina and liver (4–7). Recent studies reported another antioxidative system in which ferroptosis suppressor protein 1 at the plasma membrane provided reduced coenzyme Q₁₀ (ubiquinone-10), which effectively prevented lipid peroxidation in the absence of GPX4 (8, 9).

Ferroptosis requires intracellular labile iron, because it is suppressed by iron chelators (e.g. desferrioxamine), chemical inhibitors of lysosome function (e.g. bafilomycin A₁) and the gene silencing of transferrin receptor 1 or NCOA4, a selective cargo receptor for the autophagic degradation of ferritin (10–12). Although the exact mechanism remains elusive, iron has been suggested to catalyze Fenton-type reactions for the production of lipid radicals and the subsequent accumulation of lipid aldehydes in membranes.

The screening of small compound libraries identified ferrostatin-1 and liproxstatin-1, as specific inhibitors of ferroptosis, in addition to having lipophilic antioxidant properties related to α -tocopherol (3, 13). These amines have shown to inhibit lipid peroxidation, similar to radical-trapping antioxidants (RTAs), and nitroxides that exhibit RTA activity have recently been reported as potent ferro-

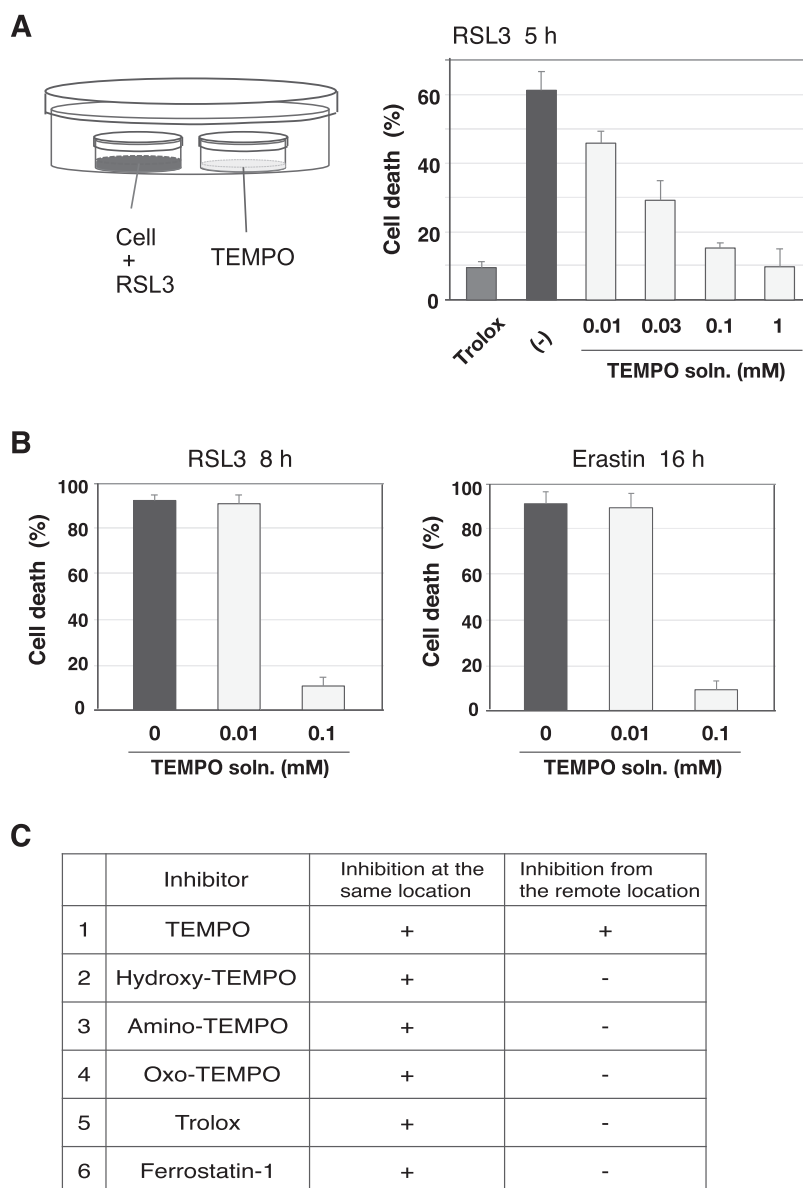


Fig. 1. Ferroptotic cell death may be prevented by TEMPO from a remote location. (A) HT1080 cells in 35 mm dishes were treated with 1 μ M RSL3 for 5 h. 10 μ l of TEMPO solution (1, 2.5, 10 and 100 mM, dissolved in DMSO) was added to 1 ml of water in different 35 mm dishes at the same time as RSL3, as shown in the illustration. Cells and water dishes were placed side by side in the 100 mm dish and were incubated at 37°C. Trolox was added to RSL3-treated cells (0.2 mM). The cell death rate was determined by the trypan blue dye-exclusion assay. Results are the mean \pm SE of three independent experiments. (B) HT1080 cells were treated with 1 μ M RSL3 (left panel) or 10 μ M erastin (right panel) in the presence or absence of the TEMPO dish for the indicated time. The cell death rate was determined as in (A). Results are the mean \pm SE of three independent experiments. (C) Summary of the inhibitory effects of various ferroptosis inhibitors. Although TEMPO, 4-hydroxy-TEMPO, 4-amino-TEMPO, 4-oxo-TEMPO, trolox and ferrostatin-1 all inhibited RSL3-induced ferroptosis in medium, only TEMPO suppressed it from a remote location (see Supplementary Fig. S1).

tosis inhibitors (14–16). 2,2,6,6-tetramethylpiperidine-1-oxyl (TEMPO) is an archetypic nitroxide. Its hydrophilic analogs, such as 4-hydroxy-TEMPO (TEMPOL), are more stable and have been investigated for pharmacological applications to the prevention of oxidative cytotoxicity in several rodent disease models (17–19).

We herein examined a number of radical scavengers for their ability to protect tumor cells from ferroptotic death, and unexpectedly noted the remote effect of TEMPO. Cerebral ischemic damage was significantly reduced in mice that inhaled this spontaneously vaporized compound. Therefore, TEMPO administered by inhalation may be

effective in the acute treatment of patients with cerebral infarction.

Materials and Methods

Inhibitors Erastin and ferrostatin-1 were purchased from Merck Calbiochem (Darmstadt, Germany). RSL3 was from Selleck Chemicals (Houston, TX). 6-Hydroxy-2,5,7,8-tetramethylchroman-2-carboxylic acid (Trolox) was purchased from Tokyo Chemical Industries (Tokyo). TEMPO was purchased from Fujifilm Wako (Osaka)

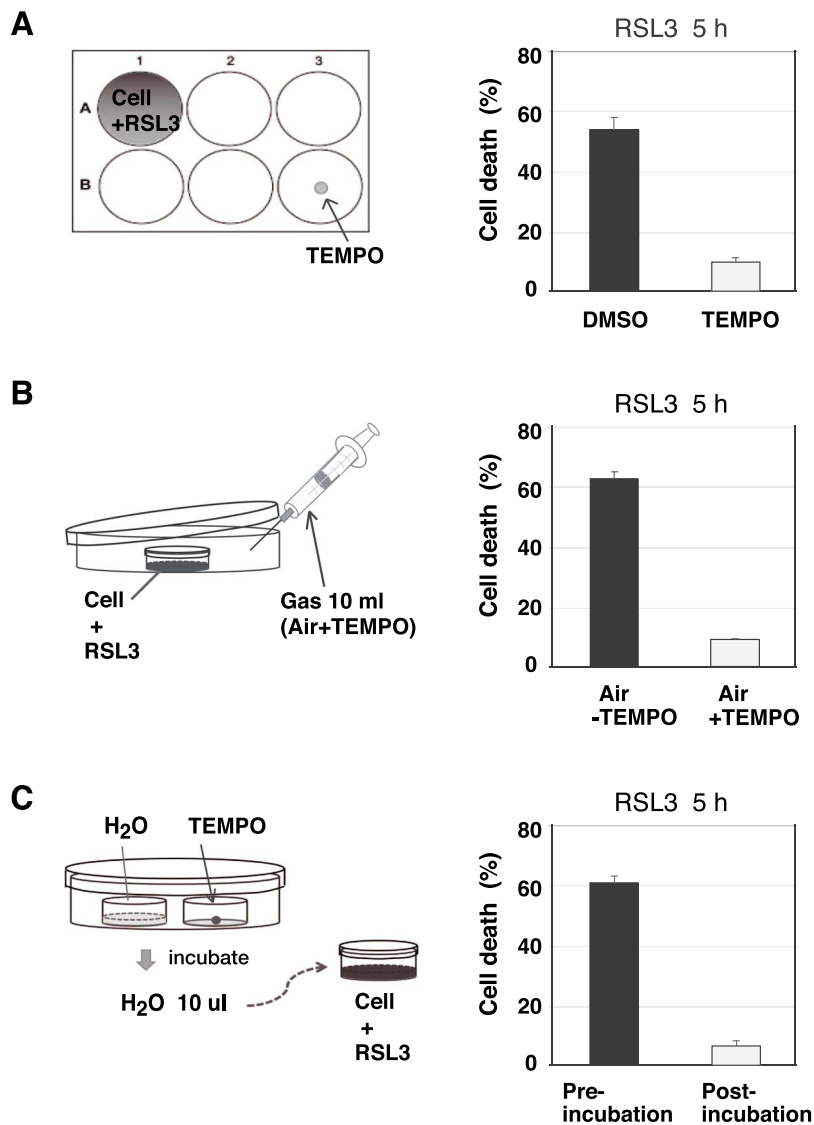


Fig. 2. TEMPO from a remote location vaporizes and then dissolves in cell medium. (A) HT1080 cells in a 6-well plate were treated with $1 \mu\text{M}$ RSL3 for 5 h. $1 \mu\text{l}$ of TEMPO (100 mM, in DMSO) or DMSO was placed in a different well at the same time as RSL3, as shown in the illustration. The cell death rate was determined by the trypan blue dye-exclusion assay. (B) $10 \mu\text{l}$ of TEMPO (100 mM, in DMSO) in a 75-mm flask was heated at 37°C , and gaseous components in air were collected. This gas was then injected into a 100 mm dish in which cells in a 35 mm dish were treated with RSL3, as shown in the illustration. The cell death rate was determined as in (A). (C) $10 \mu\text{l}$ of TEMPO (100 mM, in DMSO) and 1 ml of water were placed in separate 35 mm dishes and heated at 37°C in one 100 mm dish (sealed), as shown in the illustration. $10 \mu\text{l}$ each of water from the preincubation and post-incubation were collected and then added to RSL3-treated cells. The cell death rate was determined as in (A). All results are the mean \pm SE of three independent experiments.

and Merck Sigma (St. Louis, MO). TEMPOL, 4-amino-TEMPO, and 4-Oxo-TEMPO were purchased from Merck Sigma. Free radical scavenger MCI-186 was purchased from Cayman Chemical (Ann Arbor, MI). All chemicals were dissolved in dimethyl sulfoxide (DMSO) unless otherwise indicated.

Cell culture and cell death induction HT1080 (human fibrosarcoma) cells were cultured in Dulbecco's modified Eagle's medium (DMEM) containing 10% fetal bovine serum (FBS). For ferroptosis induction, cells were plated at 1.0×10^5 cells per well on 6-well plates or on 35 mm dishes and cultured for 40 h. Culture medium was replaced with 1 ml of medium containing erastin or RSL3 with or without inhibitors. To induce apoptosis/necrosis, cells were treated with 0.4 mM hydrogen peroxide for 12 h, tumor necrosis

factor- α (TNF- α , Fujifilm Wako) with cycloheximide for 24 h, or 25 J/m^2 UV radiation. The mouse hippocampal cell line HT22 was cultured in low glucose DMEM containing 10% FBS. Regarding the glutamate treatment, cells were plated at 1×10^5 cells per dish on 35 mm dishes, and cultured for 24 h. Culture medium was replaced with 1 ml of medium containing 5 mM glutamate. Cell viability was determined by the trypan blue dye-exclusion assay, as previously described (11).

Vaporized TEMPO treatment Ten microliters of 100 mM TEMPO was placed in a T75 flask (or 1-L aluminum bag), and the flask cap was substituted by a septum cap. After incubating TEMPO at 37°C for 3 h, 10 ml of gas including air was collected using a gas tight syringe with a Luer Lock needle (SGE Analytical Science, Melbourne). The

Table 1. Quantitative analysis of vaporization and redissolution of TEMPO.

1 ml of TEMPO stock solution (50 mM, in H₂O) and 1 ml of water were placed in separate 35-mm dishes, and both dishes were placed in a 100-mm culture plate (sealed), as shown in the illustration in Fig. 2C. After incubating the plate in CO₂ incubator at 37°C for 1 h, both reservoir (TEMPO) and receiver (water) solutions were collected and then their concentrations of TEMPO were determined by LC/MS (n = 2) or the absorption spectroscopy (n = 3)

Method	TEMPO concentration (stock reservoir) (mM)	TEMPO concentration (water receiver) (mM)
LC/MS	38.27	6.85
Absorption spectroscopy	38.50	6.80

gas was injected into a 100 mm sealed dish with a 35 mm cell culture dish placed at its center. For permanent middle cerebral artery occlusion (MCAO) mice, fresh TEMPO solution (dissolved in H₂O) in a 35 mm dish with 20 needle holes was placed in the center of the mouse cage.

Quantitation of TEMPO TEMPO was quantified by using a triple quadrupole mass spectrometer coupled with a Nexera liquid chromatograph system (LCMS-8050 system, Shimadzu). The chromatographic separation of TEMPO was conducted on a Mastro C18 column (3 μm, 2.1 × 150 mm, Shimadzu). The mobile phase consisted of 50 mM ammonium formate (pH 4.0) with methanol in 95:5 (v/v) (mobile phase A) and 5:95 (v/v) (mobile phase B) at a flow rate of 0.3 ml/min. The gradient program (time (A:B %)) was as follows: 0 min (10:90), to 0.5 min (10:90), to 5.5 min (40:60), to 6.5 min (0:100), to 8.5 min (0:100), to 9 min (10:90) and to 11 min (10:90). The column oven temperature was set at 55°C. The eluent was ionized by electrospray ionization, then measured by the mass spectrometer in selected reaction monitoring (SRM) mode. The SRM transition for TEMPO was *m/z* 157.15 [M + H]⁺ > 142.1. Peak identification and peak area integration were performed by using the LabSolutions software (Version 5.99 SP2, Shimadzu) according to the manufacturer's instructions. Nitroxides including TEMPO exhibit a weak absorption peak in the visible region (420–470 nm) in the ultraviolet–visible (UV–vis) spectra analysis (20). The absorption of the aqueous TEMPO solutions in the visible region (430 nm) was measured by a Bio-Rad SmartSpec Plus spectrophotometer, and the concentrations were calculated according to a calibration curve.

Middle cerebral artery occlusion All procedures were performed according to the rules governing animal experimentation and the guidelines for the Care and Use of Laboratory Animals, Gunma University. All mice were kept for >2 days before surgical interventions, at a 14/10 h light/dark cycle with *ad libitum* access to water and food. Adult male mice (C.B-17/Icr – +/+Jcl, 7–10 weeks, 30–35 g body weight, CREA Japan) were anesthetized with 2–5% isoflurane in O₂/air (1:9). Mice were maintained as normotensive, normocapnic, adequately oxygenated and normothermic during anesthesia. Focal cerebral ischemia was induced using a modification of the MCAO method for rats, as previously described (21). Briefly, the zygomatic bone was cut to expose the base of the temporal bone, and a 4 × 4 mm hole was made to expose the MCA. Cerebral ischemia was induced by electrocoagulation. After visually

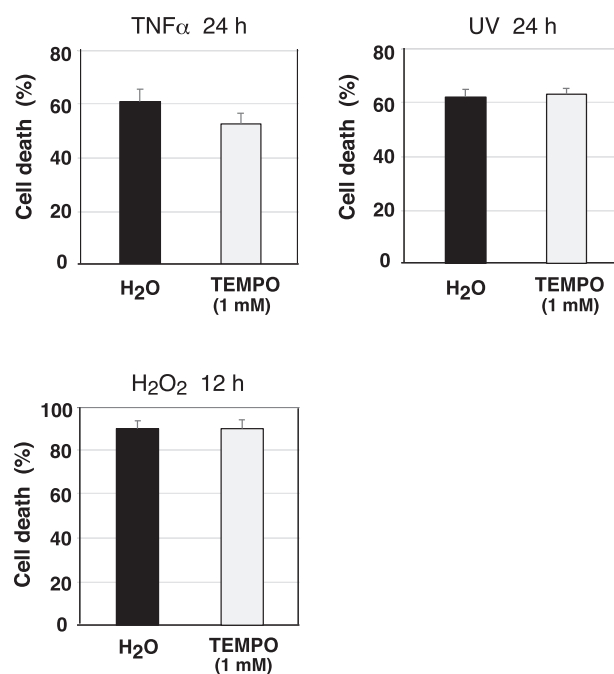


Fig. 3. Vaporized TEMPO does not affect apoptosis or necrosis. HT1080 cells were treated with 25 ng/ml tumor necrosis factor- α plus 10 μg/ml cycloheximide, 40 J/m² UV radiation or 0.1 mM hydrogen peroxide in the presence or absence of the TEMPO dish (as examined in Fig. 1A) for the indicated time. The cell death rate was determined by the trypan blue dye-exclusion assay. Results are the mean ± SE of three independent experiments.

confirming blood flow occlusion, the cauterized vessel was cut after cleaning the wound. Rectal temperature was carefully monitored during recovery from anesthesia. Fifteen minutes after infarction, mice were placed one by one in a 17 × 10 × 10 cm cage with an air hole and randomly assigned to one of the following three groups. In the control group, 0.1 g of cotton placed in a 35 mm dish was soaked with 5 ml of water and then placed in the center of the cage. In the TEMPO group, freshly made TEMPO solution (dissolved in H₂O) was used instead of water. In the MCI-186 group, 0.1 ml of MCI-186 solution (3 mg/ml) was injected into mice via the femoral vein 15 min after infarction.

Magnetic resonance imaging Magnetic resonance imaging (MRI) measurements were performed using a 1 T animal MRI scanner (ICON, Bruker, Billerica, MA, USA). T2-weighted MRI scans were obtained 3, 5 and 7 h after the MCAO treatment. To calculate the infarct level, images were analyzed with ImageJ (NIH, Bethesda, MD). The signal intensity ratio (mean value of the infarcted area/mean value of the non-infarcted area) was calculated as the ratio between the average of the measured values of three points located at a certain distance in the infarcted area and that of three points on the non-infarcted side of the infarcted area, which was linearly symmetrical.

Tissue processing and ischemic damage assessment Briefly, mice were deeply anesthetized with 5% halothane, and fixed with 50 ml of ice-cold 3.8% formaldehyde in 0.1 M sodium phosphate buffer (pH 7.4) via cardiac perfusion for 10 min after washing out blood with physiological saline for 3 min. After the perfusion of physiological saline, the brain was quickly and carefully removed, and the forebrain was sliced in eight 1-mm-thick

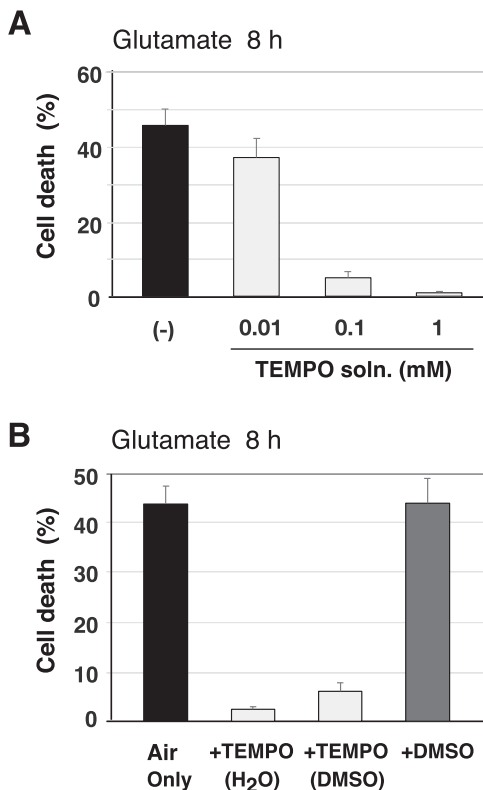


Fig. 4. Vaporized TEMPO inhibits glutamate-induced oxytosis in HT22 cells. (A) HT22 cells in a 35 mm dish were treated with 5 mM glutamate for 8 h. 10 μ l of TEMPO solution (1, 10 and 100 mM, in DMSO) were added to 1 ml of water in a different 35 mm dish at the same time as glutamate, as shown in Fig. 1A. The cell death rate was determined by the trypan blue dye-exclusion assay. Results are the mean \pm SE of three independent experiments. (B) Air containing warmed TEMPO (100 mM solution in H₂O or DMSO) or DMSO was injected into a 100 mm dish in which cells in a 35 mm dish were treated with 5 mM glutamate, as shown in Fig. 2B. The cell death rate was determined as in (A). Results are the mean \pm SE of three independent experiments.

coronal sections. Sections were treated with 2% 2,3,5-triphenyltetrazolium chloride (TTC) solution for 15 min to detect ischemic damage. Areas of brain damage were then assessed with ImageJ and integrated using the known distance between each coronal level to determine the total volume of ischemic damage in each specimen.

Statistical analysis Parametric data were compared between multiple groups by a one-way analysis of variance followed by the Tukey–Kramer test. Data are shown as the mean \pm SE. Non-parametric data were compared between the Kruskal–Wallis test followed by the Steel–Dwass test.

Results

In the process of screening for inhibitors of RSL3-induced ferroptosis using with human fibrosarcoma HT1080 cells, we noted the remote effect of TEMPO. When this compound was present in one of the 6-well plates, ferroptotic cell death was not observed in cells in the other wells, including those with the RSL3 alone, the positive control. To confirm this effect, RSL3 was added to HT1080 cells in a 35 mm dish, and TEMPO was dissolved in water in another 35 mm dish, and both were incubated together in

a 100 mm culture plate at 37°C (Fig. 1A left). TEMPO at a distance protected cells from ferroptotic death, and this protective activity was dose-dependent (Fig. 1A). Since the induction of cell death by RSL3 is rapid, the remote function may only have functioned transiently to retard ferroptotic signaling. However, we found that TEMPO (>0.1 mM) completely prevented cell death induced by RSL3 or another type inducer erastin even when incubated with cells for longer time periods (Fig. 1B).

TEMPO is multi-functional paramagnetic compound that functions as a radical or electron scavenger and its potency against ferroptosis was previously characterized by Griesser *et al.* (16). Consistent with previous findings, ferrostatin-1 and Trolox, inhibitors of lipid radical propagation and three TEMPO-related chemicals (hydroxy-, amino- and oxo-) all blocked drug-induced ferroptosis in HT1080 cells when simultaneously added to the medium (Supplementary Fig. S1) (3). However, none of these compounds were effective in separate dishes, and TEMPO was the only inhibitor that exerted its effects on cells in a remote manner (Fig. 1C and Supplementary Fig. S1). We then investigated the mechanisms by which TEMPO acts on cells from the remote locations. The same inhibitory effect was observed in 6-well plates using a small volume (1–2 μ l) of 0.1 M TEMPO (Fig. 2A). During this experiment, we detected a slightly pungent smell emanating from the plate. Furthermore, ferroptotic cell death was inhibited by an injection of the collected air after the solution was maintained at 37°C for 3 h, suggesting that TEMPO acts on cells by vaporization (Fig. 2B). Heated TEMPO was then analyzed by gas chromatography-mass spectrometry (GC/MS), and the results obtained confirmed that the major gas component was TEMPO itself (Supplementary Fig. S2). When pure water and the TEMPO solution in separate dishes were heated side by side, water after 3 h completely inhibited cell death (Fig. 2C). These results suggest that TEMPO vaporized into air, and some of the gas dissolved in the culture medium and acted as a radical scavenger. To estimate the amount of the transferred TEMPO, we measured the concentration of TEMPO in reservoir and receiver by liquid chromatography-mass spectrometry (LC/MS) and the absorption spectroscopy. The results indicated that 23% of TEMPO dissolved in water (50 mM) vaporized, while approximately 14% moved into a nearby water after a 1-h incubation at 37°C (Table 1).

We investigated whether TEMPO inhibits different types of cell death under the same conditions. TEMPO (1 mM) did not inhibit cell death induced by TNF- α , UV radiation or hydrogen peroxide (Fig. 3). These results suggest that TEMPO vapor gas did not affect apoptosis or necrosis. Since oxidative cell death in neurons, called oxytosis, is related to ferroptosis (22, 23), we examined the effects of TEMPO gas on glutamate-induced oxidative toxicity in the hippocampal cell line HT22. As shown in Fig. 4A, TEMPO remotely prevented cells death in HT22 cells at similar concentrations to those that inhibited ferroptosis in cancer cells. Similarly, the injection of air containing vaporized TEMPO was sufficient to block glutamate-induced toxicity (Fig. 4B).

The effects of TEMPO were evaluated *in vivo* using a mouse ischemia model. We generated permanent MCAO

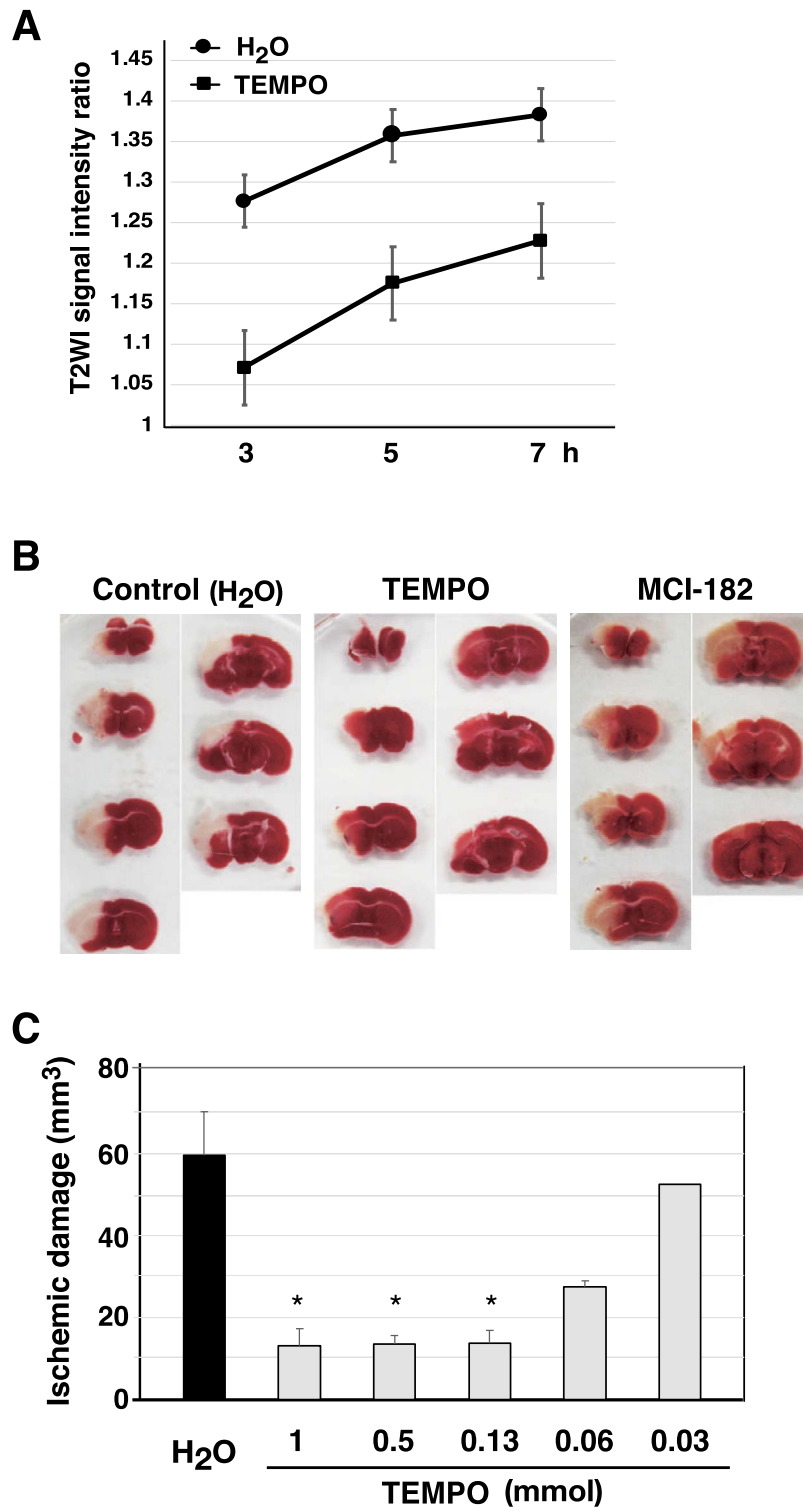


Fig. 5. Volatile TEMPO protects neuronal cells from ischemia. (A) 3, 5 and 7 h after MCAO, T2-weighted images (T2WI) were obtained using MRI. Signal intensity ratios (mean value of the infarcted area/mean value of the non-infarcted area) were represented ($n = 3$). (B) 8 h after MCAO, ischemic damage was detected using TTC staining. In TTC-stained slices, infarcted tissue appeared white, while intact tissue stained in color. (C) The infarct volume was measured and represented by the mean \pm SE of three independent experiments. * $P < 0.05$; one-way analysis of variance followed by the Tukey–Kramer test.

for focal cerebral ischemia in mice and examined whether the inhalation of TEMPO gas attenuated neural damage. Similar to the results obtained in the experiments with cells, various concentrations of TEMPO solution in 35 mm dishes were placed in the center of the mouse cage, and

the inhalation effects of its spontaneous evaporation were assessed. T2-weighted images of MRI were acquired 3, 5 and 7 h after MCAO, and the intensity of the infarct area was significantly lower with the TEMPO treatment than with the water control (Fig. 5A). Furthermore, the volume

of infarction in gray and white matter shown by TTC staining was reduced in mice treated by TEMPO, which was markedly smaller than that in MCI-186-injected mice (Fig. 5B). The infarct volume was 77% less with TEMPO at concentrations higher than 0.125 mmol than with the water control, and the suppression of neural damage was dependent on the concentration of TEMPO solution (Fig. 5C). These results suggest that following its inhalation, TEMPO gas quickly moved into the cerebrum and specifically protected neural cells in mice.

Discussion

Oxidative toxicity in neural cells has been implicated in degenerative neuronal diseases, intracerebral hemorrhage and cerebral ischemia (22). In the pathogenesis of cerebral infarction, a model system using the mouse hippocampal HT22 cell line is useful for elucidating the mechanisms underlying oxidative stress-induced neuronal cell death. In oxytosis, a treatment with glutamate depletes GSH, resulting in increases in ROS, which also occurs in one form of ferroptosis. The signaling pathway involved in the two types of cell death are similar, featuring the lysosome-mediated provision of iron, 15-lipoxygenase activity, and the generation of lipid hydroperoxide; however, some differences were recently reported (24, 25). The present results indicated that the nitroxide radical TEMPO prevented oxytosis and ferroptosis in a remote manner. Furthermore, neural damage in MCAO mice was markedly reduced in an environment in which TEMPO naturally vaporized.

We demonstrated that ferroptosis and oxytosis were completely prevented by a treatment with some of the vapor gas collected from warmed TEMPO (Figs 2B and 4B). Moreover, when water in a separate dish from the TEMPO solution was heated in a sealed container, it exhibited inhibitory activity against cell death (Fig. 2C). Analysis of a gas and solution by GC/MS and LC/MS, respectively, revealed that TEMPO was volatilized intact without being decomposed and redissolved in a nearby water (Table I and Supplementary Fig. S2).

Nitroxyl radicals including TEMPO are well-known ROS scavengers and have been shown to protect neurons from traumatic brain injury and cerebral ischemia in rodent models (17–19). In contrast to TEMPO, its analogs, such as TEMPOL, and several other lipophilic ferroptosis/oxytosis inhibitors did not affect RSL3-induced ferroptosis from a remote location (Fig. 1C). These results suggest that TEMPO possesses unique physical properties for volatility. The initial study of ferroptosis mentioned the blocking effect of TEMPO (3), and the mechanism underlying its inhibitory effects on lipid peroxidation was recently elucidated (16). The main result of the present study is the potent volatility-mediated effects of TEMPO on remote samples; however, it currently remains unclear whether the inhibitory mechanism is the same.

Our experiments using the permanent MCAO mouse model suggested that TEMPO vapor gas is protective *in vivo* against cerebral ischemia, in which lipid peroxidation has been implicated. The infarct volume was significantly reduced by inhalation treatments of vaporized TEMPO in a dose-dependent manner (Fig. 5C). Furthermore, immunos-

taining for a major aldehyde product of lipid peroxidation, 4-hydroxy-2-nonenal, revealed its low accumulation in the infarcted area in TEMPO-treated MCAO mice (Supplementary Fig. S3). Brain damage associated with cerebral ischemia and reperfusion involves oxidative stress caused by ROS (22), and MCI-186 (also known as edaravone), a free radical scavenger, is the only approved drug that exerts brain protective effects. Other compounds that reduce oxidative stress have also been examined. Therefore, the present results are important, and cerebral protection by TEMPO inhalation may be an effective treatment for ischemic insults at the post-infarct emergency phase.

Supplementary Data

Supplementary Data are available at *JB* Online.

Funding

This work was supported by Grants-in-Aid from the Japanese Society for the Promotion of Science (JSPS) (17K08528 and 19 K07814), Grant for Basic Science Research Projects from the Sumitomo Foundation, the Japan Arteriosclerosis Prevention Research Fund and the collaborative research project (#20007) of the Brain Research Institute, Niigata University.

Acknowledgements

The authors thank Drs S. Matsuzawa (Kyoto University), T. Takeuchi, K. Sato, I. Amano, K. Yamada, H. Horiuchi and T. Yoshihara (Gunma University) for technical advice and helpful discussion. We also thank Ms R. Torii and Ms M. Yamakawa for their generous support.

Conflict of Interest

None declared.

REFERENCES

1. Stockwell, B.R., and Jiang, X.J. (2020) The chemistry and biology of ferroptosis. *Cell Chem. Biol.* **27**, 365–375
2. Zheng, J.S., and Conrad, M. (2020) The metabolic underpinnings of ferroptosis. *Cell Metab.* **32**, 920–937
3. Dixon, S.J., Lemberg, K.M., Lamprecht, M.R., Skouta, R., Zaitsev, E.M., Gleason, C.E., Patel, D.N., Bauer, A.J., Cantley, A.M., Yang, W.S., Morrison, B., and Stockwell, B.R. (2012) Ferroptosis: an iron-dependent form of nonapoptotic cell death. *Cell* **149**, 1060–1072
4. Seiler, A., Schneider, M., Forster, H., Roth, S., Wirth, E.K., Culmsee, C., Plesnila, N., Kremmer, E., Radmark, O., Wurst, W., Bornkamm, G.W., Schweizer, U., and Conrad, M. (2008) Glutathione peroxidase 4 senses and translates oxidative stress into 12/15-lipoxygenase dependent- and AIF-mediated cell death. *Cell Metab.* **8**, 237–248
5. Ueta, T., Inoue, T., Furukawa, T., Tamaki, Y., Nakagawa, Y., Imai, H., and Yanagi, Y. (2012) Glutathione peroxidase 4 is required for maturation of photoreceptor cells. *J. Biol. Chem.* **287**, 7675–7682
6. Carlson, B.A., Tobe, R., Yefremova, E., Tsuji, P.A., Hoffmann, V.J., Schweizer, U., Gladyshev, V.N., Hatfield, D.L., and Conrad, M. (2016) Glutathione peroxidase 4 and vitamin E cooperatively prevent hepatocellular degeneration. *Redox Biol.* **9**, 22–31
7. Hambright, W.S., Fonseca, R.S., Chen, L.J., Na, R., and Ran, Q.T. (2017) Ablation of ferroptosis regulator glutathione peroxidase 4 in forebrain neurons promotes cognitive impairment and neurodegeneration. *Redox Biol.* **12**, 8–17

8. Bersuker, K., Hendricks, J.M., Li, Z.P., Magtanong, L., Ford, B., Tang, P.H., Roberts, M.A., Tong, B.Q., Maimone, T.J., Zoncu, R., Bassik, M.C., Nomura, D.K., Dixon, S.J., and Olzmann, J.A. (2019) The CoQ oxidoreductase FSP1 acts parallel to GPX4 to inhibit ferroptosis. *Nature* **575**, 688–692
9. Doll, S., Freitas, F.P., Shah, R., Aldrovandi, M., da Silva, M.C., Ingold, I., Grocin, A.G., da Silva, T.N.X., Panzilius, E., Scheel, C.H., Mourao, A., Buday, K., Sato, M., Wanning, J., Vignane, T., Mohana, V., Rehberg, M., Flatley, A., Schepers, A., Kurz, A., White, D., Sauer, M., Sattler, M., Tate, E.W., Schmitz, W., Schulze, A., O'Donnell, V., Proneth, B., Popowicz, G.M., Pratt, D.A., Angeli, J.P.F., and Conrad, M. (2019) FSP1 is a glutathione-independent ferroptosis suppressor. *Nature* **575**, 693–698
10. Yang, W.S., and Stockwell, B.R. (2008) Synthetic lethal screening identifies compounds activating iron-dependent, nonapoptotic cell death in oncogenic-RAS-harboring cancer cells. *Chem. Biol.* **15**, 234–245
11. Torii, S., Shintoku, R., Kubota, C., Yaegashi, M., Torii, R., Sasaki, M., Suzuki, T., Mori, M., Yoshimoto, Y., Takeuchi, T., and Yamada, K. (2016) An essential role for functional lysosomes in ferroptosis of cancer cells. *Biochem. J.* **473**, 769–777
12. Gao, M.H., Monian, P., Pan, Q.H., Zhang, W., Xiang, J., and Jiang, X.J. (2016) Ferroptosis is an autophagic cell death process. *Cell Res.* **26**, 1021–1032
13. Angeli, J.P.F., Schneider, M., Proneth, B., Tyurina, Y.Y., Tyurin, V.A., Hammond, V.J., Herbach, N., Aichler, M., Walch, A., Eggenhofer, E., Basavarajappa, D., Radmark, O., Kobayashi, S., Seibt, T., Beck, H., Neff, F., Esposito, I., Wanke, R., Forster, H., Yefremova, O., Heinrichmeyer, M., Bornkamm, G.W., Geissler, E.K., Thomas, S.B., Stockwell, B.R., O'Donnell, V.B., Kagan, V.E., Schick, J.A., and Conrad, M. (2014) Inactivation of the ferroptosis regulator Gpx4 triggers acute renal failure in mice. *Nat. Cell Biol.* **16**, 1180–1191
14. Krainz, T., Gaschler, M.M., Lim, C., Sacher, J.R., Stockwell, B.R., and Wipf, P. (2016) A mitochondrial-targeted nitroxide is a potent inhibitor of ferroptosis. *ACS Cent. Sci.* **2**, 653–659
15. Shah, R., Margison, K., and Pratt, D.K. (2017) The potency of diarylamine radical-trapping antioxidants as inhibitors of ferroptosis underscores the role of autoxidation in the mechanism of cell death. *ACS Chem. Biol.* **12**, 2538–2545
16. Griesser, M., Shah, R., Van Kessel, A.T., Zilka, O., Haidasz, E.A., and Pratt, D.A. (2018) The catalytic reaction of nitroxides with peroxy radicals and its relevance to their cytoprotective properties. *J. Am. Chem. Soc.* **140**, 3798–3808
17. BeitYannai, E., Zhang, R.L., Trembovler, V., Samuni, A., and Shohami, E. (1996) Cerebroprotective effect of stable nitroxide radicals in closed head injury in the rat. *Brain Res.* **717**, 22–28
18. Rak, R., Chao, D.L., Pluta, R.M., Mitchell, J.B., Oldfield, E.H., and Watson, J.C. (2000) Neuroprotection by the stable nitroxide Tempol during reperfusion in a rat model of transient focal ischemia. *J. Neurosurg.* **92**, 646–651
19. Hosoo, H., Marushima, A., Nagasaki, Y., Hirayama, A., Ito, H., Puentes, S., Mujagic, A., Tsurushima, H., Tsuruta, W., Suzuki, K., Matsui, H., Matsumaru, Y., Yamamoto, T., and Matsumura, A. (2017) Neurovascular unit protection from cerebral ischemia-reperfusion injury by radical-containing nanoparticles in mice. *Stroke* **48**, 2238–2247
20. Nakahara, K., Iwasa, S., Iriyama, J., Morioka, Y., Suguro, M., Satoh, M., and Cairns, E.J. (2006) Electrochemical and spectroscopic measurements for stable nitroxyl radicals. *Electrochim. Acta* **52**, 921–927
21. Kubota, C., Torii, S., Hou, N., Saito, N., Yoshimoto, Y., Imai, H., and Takeuchi, T. (2010) Constitutive reactive oxygen species generation from autophagosome/lysosome in neuronal oxidative toxicity. *J. Biol. Chem.* **285**, 667–674
22. Lewerenz, J., Ates, G., Methner, A., Conrad, M., and Maher, P. (2018) Oxytosis/ferroptosis-(re-)emerging roles for oxidative stress-dependent non-apoptotic cell death in diseases of the central nervous system. *Front. Neurosci.* **12**, 214
23. Ratan, R.R. (2020) The chemical biology of ferroptosis in the central nervous system. *Cell Chem. Biol.* **27**, 479–498
24. Zille, M., Kumar, A., Kundu, N., Bourassa, M.W., Wong, V.S.C., Willis, D., Karuppagounder, S.S., and Ratan, R.R. (2019) Ferroptosis in neurons and cancer cells is similar but differentially regulated by histone deacetylase inhibitors. *Eneuro* **6**, e0263
25. Soriano-Castell, D., Currais, A., and Maher, P. (2021) Defining a pharmacological inhibitor fingerprint for oxytosis/ferroptosis. *Free Radic. Biol. Med.* **171**, 219–231